Symmetrical Transformer for Medium-Voltage Medium-Frequency ISOP Three-Phase LLC SST

Mirzadarani, R.; Li, Z.; Qin, Z.; Vaessen, P.; Bauer, P.; Niasar, M. Ghaffarian

DOI
10.1109/IPEMC-ECCEAsia60879.2024.10567857

Publication date
2024

Document Version
Final published version

Published in
2024 IEEE 10th International Power Electronics and Motion Control Conference, IPEMC 2024 ECCE Asia

2024 IEEE 10th International Power Electronics and Motion Control Conference (IPEMC2024-ECCE Asia) | 979-8-3503-5133-0/24/$31.00 ©2024 IEEE | DOI: 10.1109/IPEMC-ECCEAsia60879.2024.10567857

Symmetrical Transformer for Medium-Voltage Medium-Frequency ISOP Three-Phase LLC SST

R. Mirzadarani[1], Z. Li[1], Z. Qin[1], P. Vaessen[1], P. Bauer[1], M. Ghaffarian Niasar[1]
[1] Dept. Electrical Sustainable Energy (ESE), TU Delft, The Netherlands

***Abstract*- Resonant converters are popular in power electronics due to their soft-switching capabilities, which enhance efficiency and prolong component lifetime. Three-phase resonant converters are particularly noteworthy for their higher power density and reduced ripple, making them ideal for demanding applications. A critical aspect of optimizing three-phase LLC resonant converters is the design of a transformer with adequate leakage inductance required for the resonance circuit. This paper compares two distinct transformer designs for such converters: a five-limb shell-type transformer and a symmetrical triangular transformer. Both designs are evaluated in terms of their performance, efficiency, and suitability for integration into the converter architecture. A detailed design procedure using Finite Element Method (FEM) analysis is presented to guide the development of these transformers. The practicality of this approach and its effectiveness are demonstrated through the implementation of a 3.4 kV to 60 V, 50 kVA prototype. This work provides a comparative analysis of transformer designs and introduces a validated methodology for improving the performance of three-phase LLC resonant converters through optimized transformer design.[1]**

***Index Terms*- FEM, LLC Resonant Converter, Three-Phase Transformer.**

I. Introduction

Green hydrogen is defined as hydrogen produced by splitting water into hydrogen and oxygen using renewable energy sources. Green hydrogen is increasingly recognized for its potential to revolutionize the energy landscape. However, green hydrogen production presents unique challenges, including the need for highly efficient and reliable energy conversion processes. In this context, the role of solid-state transformers becomes crucial. Because of their high efficiency and robust performance, SSTs can play an important role in refining the energy conversion processes essential for producing green hydrogen. SSTs offer superior control and flexibility compared to traditional transformers, enabling more efficient handling of the variable power inputs typical in renewable energy systems. SST enables more effective use of renewable energy sources by improving energy management in green hydrogen systems. Their integration into the infrastructure of green hydrogen production is a crucial indicator of progress in our journey towards a more sustainable and sustainable future.

Solid-state transformers (SSTs) and their use for modern renewable energy applications have been a topic of research over the past few decades [1-3]. There are different topologies for the SST's DC/DC converter, such as modular multi-level converters (MMC), dual active bridge (DAB), and resonant converters. Resonant converters offer significant advantages and are widely used in various applications nowadays [4]. The ability to eliminate switching losses, facilitated by the soft-switching feature, results in higher efficiency and power density [5]. LLC resonant converter is a well-known topology that can utilize the leakage inductance of the transformer as the required series inductance of the resonant tank if the transformer is precisely designed [4, 6-9]. Three-phase resonant converters have been the subject of several studies due to their soft-switching capability and higher power density, typical of a three-phase converter [10-12]. Nevertheless, designing and fabricating a three-phase transformer with integrated magnetic components for the resonant tank poses several challenges.

Fig. 1 shows the topology of the current study, which is an Input-Series, Output-Parallel, Three-Phase LLC (ISOP-3ph-LLC). The primary objective of this paper is to design and build a symmetrical three-phase transformer and compare it with an alternative solution, a five-limb shell-type transformer. While this type of transformer has been studied in several references [13, 14], employing this structure as a medium-frequency transformer (MFT) for a 3ph-ISOP-LLC is a novel application that is investigated in this paper. The comparative analysis aims to demonstrate that the proposed symmetrical three-phase transformer provides nearly equal leakage and magnetizing inductances for the LLC resonant tanks. Additionally, the proposed transformer is highlighted as lighter, smaller and more cost-effective than the conventional transformers.

Accordingly, the present paper is organized as follows. Section II introduces the input-series output-parallel three-phase LLC (ISOP-3ph-LLC). Section III gives information about the proposed symmetrical three-phase transformer. Section IV provides the simulation results, and section V includes the experimental results and comparison. Finally, section VI concludes the paper.

This project has received funding from the RVO MOOI (Missiegedreven Onderzoek Ontwikkeling en Innovation) under grant agreement MOOI 52103.

II. Input-Series Output-Parallel Three-Phase LLC

The ISOP converter can handle a relevantly high voltage on the primary side due to the series connection of the primaries, as well as a high current on the secondary side owing to the parallel outputs [15-17]. Therefore, this topology is ideal for step-down applications, such as supplying power to a high-current load like a hydrogen electrolyzer from a high- or medium-voltage grid. The converter of the present study is a down-scaled prototype intended for an MVA-scaled 33 kV SST system under development for green hydrogen production. The optimum frequency for the actual SST is 1 kHz; therefore, the frequency of the converter in the present paper is selected as 1 kHz. The DC bus voltage is 3.4 kV, and the converter has four three-phase transformers, each rated at 12.5 kVA. The converter is designed to withstand a 10 kV AC voltage test. The characteristics of the prototype converter are summarized in Table I. To ensure balanced operation and prevent circulating current, the LLC modules shown in Fig. 1 must be constructed as similarly as possible. Therefore, the leakage inductances of the windings for each phase must be as equal as possible (Fig. 2).

voltage unbalance can significantly impact transformer performance, leading to a series of detrimental effects such

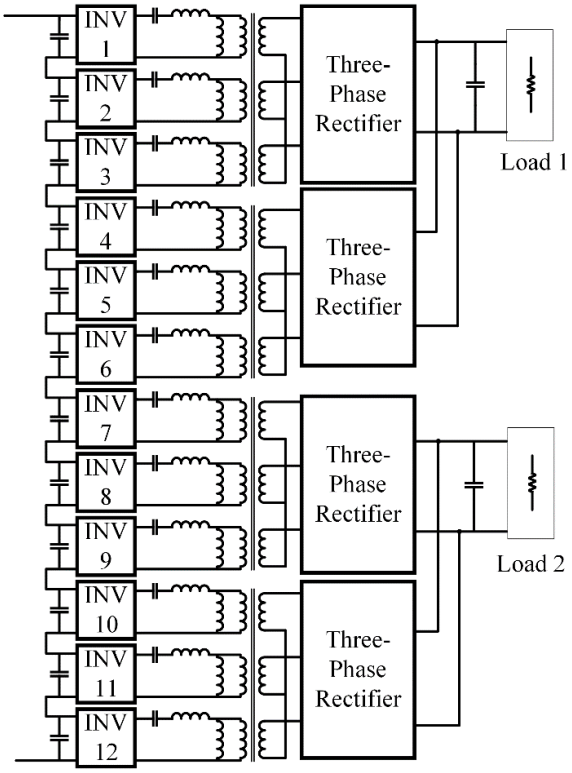

Fig. 1. Schematic of the ISOP 3ph LLC SST.

Table I
Characteristics of the Prototype Converter

Parameter	Symbol	Unit	Value
Input voltage	V_{in}	kV	3.4
Output voltage	V_{out}	V	60
Rating power	S	kVA	50
Rating power of each transformer	P_{tr}	kVA	12.5
Frequency	f	kHz	1

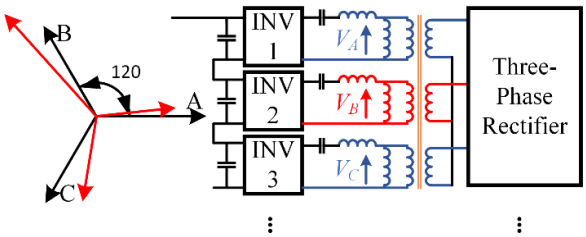

Fig. 2. Unbalanced situation in the three-phase LLC converter.

as increased losses, overheating, and degradation of insulation life, thus compromising system efficiency and reliability. Specifically, in the context of three-phase LLC resonant converters, where primary side inverters are series-connected, ensuring uniform leakage inductance across each phase becomes paramount. This uniformity is crucial because discrepancies in leakage inductance can lead to unequal voltage distribution across the transformers' phases, exacerbating the aforementioned issues by inducing additional currents that can distort the system's output and stress electronic components. Therefore, meticulous design considerations must be employed to guarantee that the transformer's leakage inductances are as similar as possible, thereby ensuring balanced voltage conditions. This approach not only enhances the overall system performance but also prolongs the operational lifespan of the transformer and connected devices, reinforcing the necessity for precision in the design and manufacturing stages of three-phase LLC resonant converters.

The switching frequency of the LLC resonant converter is designed as follows [4]

$$f_s = \frac{1}{2\pi\sqrt{L_s C_s}} \tag{1}$$

where L_s and C_s are the series inductance and capacitance of the resonant tank, respectively. Since the frequency of the resonant converter is fixed for all submodules, it is essential to have series inductances that are as equal as possible in the resonant tank. In order to decrease the number of elements, the leakage inductance of the MFT is used as the L_s.

III. Symmetrical Three-Phase Transformer

A three-phase transformer can be constructed using three single-phase transformers connected in either star or delta configuration. However, this arrangement is not advantageous because an integrated three-phase transformer offers higher power density than three single-phase transformers connected individually [18]. The three-phase core-type, shell-type, and proposed symmetrical transformer are shown in Fig. 3.

An ISOP-3ph-LLC made of core-type configuration is unsuitable because the inner winding in the central leg exhibits different characteristics than the other windings, resulting in an imbalance. The transformer is designed as follows. The number of turns should be selected as low as possible to minimize the load loss [18]. Although the primary voltage is 3.4 kV, each winding experiences 283 V due to the series connection of the inputs. However, the

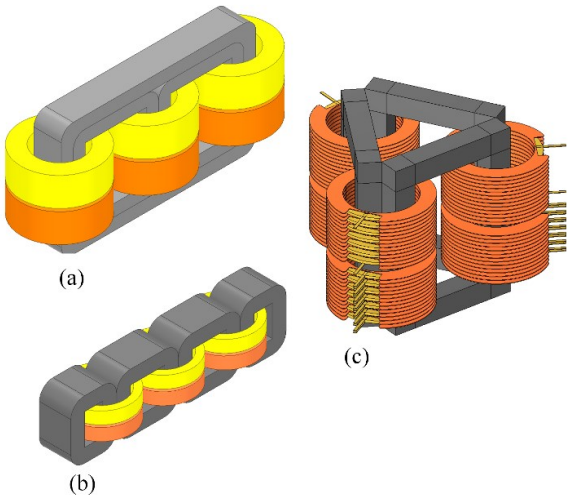

Fig. 3. a) Core-type, b)shell-type, and c) proposed symmetrical transformers.

peak value of the input voltage reaches up to 318 V because of the presence of resonant tank elements. The required core cross-section area is calculated as follows:

$$A_c = \frac{E_{peak} \times t}{2 \times N_p \times B_m} \tag{2}$$

where E_{peak} is the peak value of the primary voltage, t is the duty cycle, N_p is the number of turns on the primary side, and B_m is the maximum flux density. The core material is ferrite BFM8; thus, B_m = 190 mT. The transfer ratio is 8.5, resulting in N_p = 85 and N_s = 10. According to (2), the core cross-sectional area A_c can be calculated as 3200 mm^2. In the proposed symmetrical three-phase transformer, the core consists of 6 commercially available U240/160/40 ferrite cores connected in a triangular configuration. The proposed transformer ensures a leakage inductance similar to sell-type transformers but with lesser weight, as it utilizes six U-cores instead of eight. The primary and secondary are on top of each other to maintain a certain amount of leakage inductance for the resonant converter. In this way, no additional series inductance is needed, which benefits the converter's power density.

The conductors of the proposed transformer are selected based on the currents and the frequency. The skin depth can be calculated as follows:

$$\delta = \sqrt{\frac{2\rho}{\omega\mu}} \tag{3}$$

where ρ, ω, and μ are resistivity, angular frequency, and permeability, respectively. Since the conductor is made of copper and the frequency of the converter is 1 kHz, the skin depth is calculated as 2.06 mm. Therefore, a 5×1 mm rectangular enamelled conductor is selected to build both primary and secondary. The rectangular conductors are also better to make a disk winding. The primary has 85 turns, and the secondary has 10 turns. However, because of the higher current on the secondary side, the secondary is made of 7 parallel paths. Both primary and secondary are disk windings. Primary has 13 disks. Disks number 1, 3, 7, 11, and 13 have 11 turns (disk type 1), disks number 5 and 9 have 12 turns (disk type 2), and disks number 2, 4, 6, 8, 10, and 12 have one turn (disk type 3) to maintain the required distance between disks. The mean length of turns for these disks is as follows:

$$MLT_{p\_i} = \pi \times (D_{in} + W_i) \tag{4}$$

$$MLT_s = \pi \times (D_{in} + W_s) \tag{5}$$

where D_{in} is the inner diameter of the bobbin (=130 mm), and W_i is the widths of disk types 1 to 3, respectively. W_s is the width of the secondary disk. Consequently, the primary and secondary lengths can be calculated as l_p = 37.8 m/phase and l_s = 4.4 m/phase, respectively. The AC resistance per unit length of each winding is obtained from a 2D COMSOL simulation. Accordingly, R_{ac} can be calculated as:

$$R_{ac\_p} = r_{ac\_p} \times l_p \quad , \quad R_{ac\_s} = r_{ac\_s} \times l_s \tag{6}$$

where r_{ac_p} and r_{ac_s} are the ac resistance per unit length of the primary and secondary, respectively; consequently, the copper loss can be calculated as follows:

$$P_{cu} = 3 \times R_{ac\_p} \times I_p^2 + 3 \times R_{ac\_s} \times I_s^2 \tag{7}$$

where I_p and I_s are the primary and secondary currents, respectively. It is noteworthy that the secondary has 7 disks, which are connected in parallel. There is more distance between secondary disks to provide sufficient space for connections to the high-current busbar.

IV. Simulation

To prove the mathematical calculations, a Finite Element Method (FEM) simulation is performed using ANSYS Maxwell 3D, as shown in Fig. 4. The leakage inductance is calculated as follows:

$$L = \begin{pmatrix} L_{11} & L_{12} & L_{13} \\ L_{21} & L_{22} & L_{23} \\ L_{31} & L_{32} & L_{33} \end{pmatrix} \tag{8}$$

$$L_{lk\_n} = L_{nn} - \frac{L_{nm} \times L_{mn}}{L_{mm}} \tag{9}$$

where L_{nn}, L_{nm}, L_{mn}, and L_{mm} are the elements of the inductance matrix from ANSYS Maxwell. The simulation results are summarized in TABLE II and compared with the experimental results.

V. Experimental Results and Comparison

This section compares a symmetrical three-phase transformer and a conventional five-limb shell-type

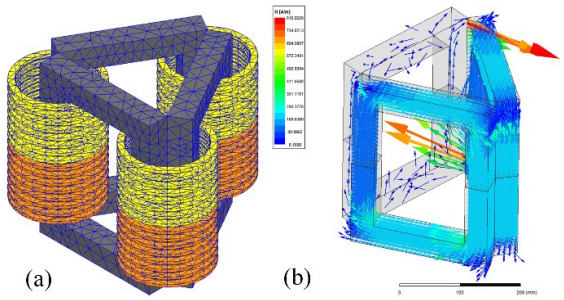

Fig. 4. a) The mesh performance of FEM simulation, b) H-vectors inside the core caused by excitation of one phase.

transformer, specifically designed for a 50 kVA, 3.4 kV to 60 V DC/DC converter.

A. Setup description

The experimental setup was designed to compare these two transformer architectures. Both transformers were constructed using PLA-based 3D printed bobbins, a method that ensures precision and consistency in the winding process. This construction technique, depicted in Fig. 5, employed rectangular enamelled copper conductors measuring 1×5 mm, chosen for their efficiency and reliability. The detailed structure of the transformer is illustrated in Fig. 6.

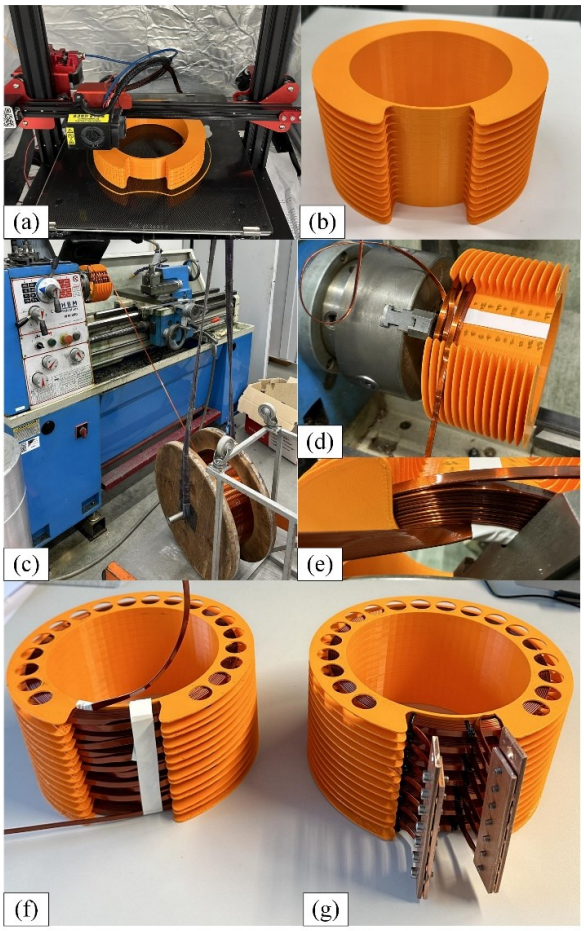

Fig. 5. The winding manufacturing process: a) 3D printing of the bobbin, b) the prepared bobbin, c) winding process, d) disk winding structure, e) details of one disk, f) the primary disk, and g) the secondary winding

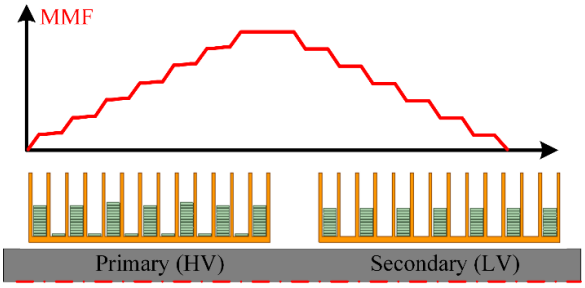

Fig. 6. Transformer structure.

The constructed transformers, the five-limb and the symmetrical types are showcased in Fig. 7, highlighting the physical differences and design approaches. It is noteworthy that these transformers are not optimized since the idea of this study is to show the difference between two configurations using the same cores and windings. Each transformer was subjected to a series of tests to assess its performance characteristics. Key measurements were conducted using a Bode 100 network analyzer.

B. Measurement

The measuring setup is shown in Fig. 8. Measurements are performed using the procedure described in [19]. The model which is used for each phase is shown in Fig. 9. The magnetizing inductance is calculated as follows:

$$L_{MAG1} = \frac{G \times a}{\omega} \sqrt{R_1^2 + \left(\omega L_1\right)^2} \tag{10}$$

$$L_{l1} = L_1 - L_{MAG1} \tag{11}$$

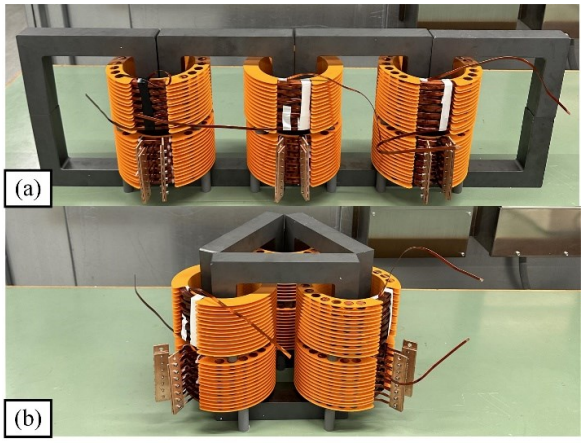

Fig. 7. a) The conventional five-limb transformer and b) the proposed symmetrical transformer

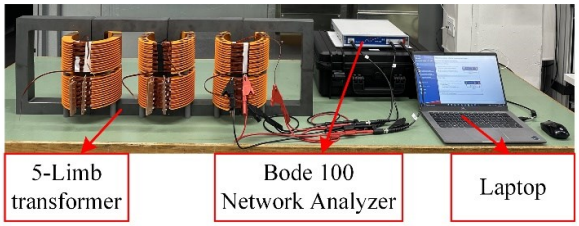

Fig. 8. Measuring setup.

TABLE II
SUMMARY OF THE RESULTS

Parameter		Magnetizing Inductance (mH)			Leakage Inductance (mH)			Weight (kg)
		L_{m1}	L_{m2}	L_{m3}	L_{LK1}	L_{LK2}	L_{Lk3}	
Prop.	FEM	47.14			2.863			33.96
	Meas.	48.67	49.22	47.21	2.669	2.754	2.668	
5 Limb	FEM	51.75	55.32	51.75	2.783	2.805	2.783	41.33
	Meas.	51.19	52.84	50.46	2.596	2.715	2.615	

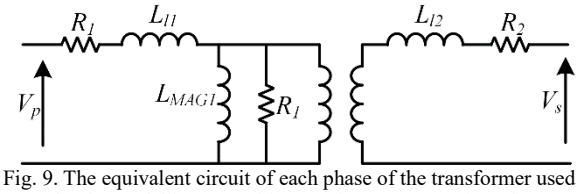

Fig. 9. The equivalent circuit of each phase of the transformer used for the modelling (parasitic capacitances are neglected).

$$L_{MAG2} = L_{MAG1} \times \left(\frac{N_s}{N_p}\right)^2 \tag{12}$$

$$L_{l2} = L_2 - L_{MAG2} \tag{13}$$

where G is the gain and a is the transfer ratio. The measured charts are shown in Fig. 10.

The results of these measurements are summarized in TABLE II referred to the primary side. Through this experimental analysis, the study aims to provide the feasibility and performance of the symmetrical three-phase transformer compared to the traditional five-limb shell-type transformer, thereby informing future design and application choices in the realm of medium-voltage, medium-frequency solid-state transformers.

VI. CONCLUSIONS

This paper presented an analysis and comparison of an innovative transformer design for use in medium-voltage, medium-frequency, Input-Series Output-Parallel Three-Phase LLC Solid-State Transformers. The primary focus was evaluating a symmetrical three-phase transformer against a conventional five-limb shell-type transformer. Through Finite Element Method (FEM) analysis and experimental validation with a 3.4 kV to 60 V, 50 kVA prototype, the study demonstrated the superior performance of the symmetrical transformer design in terms of power density and integration into solid-state transformer systems.

Key findings include the symmetrical transformer's ability to provide nearly equal leakage and magnetizing inductances for the LLC resonant tanks, which is crucial for balanced operation of the LLC resonant converter. Furthermore, the proposed transformer design was lighter, smaller, and more cost-effective than the five-limb shell-type transformer. The proposed symmetrical transformer saves 17.8% of size compared to the five-limb

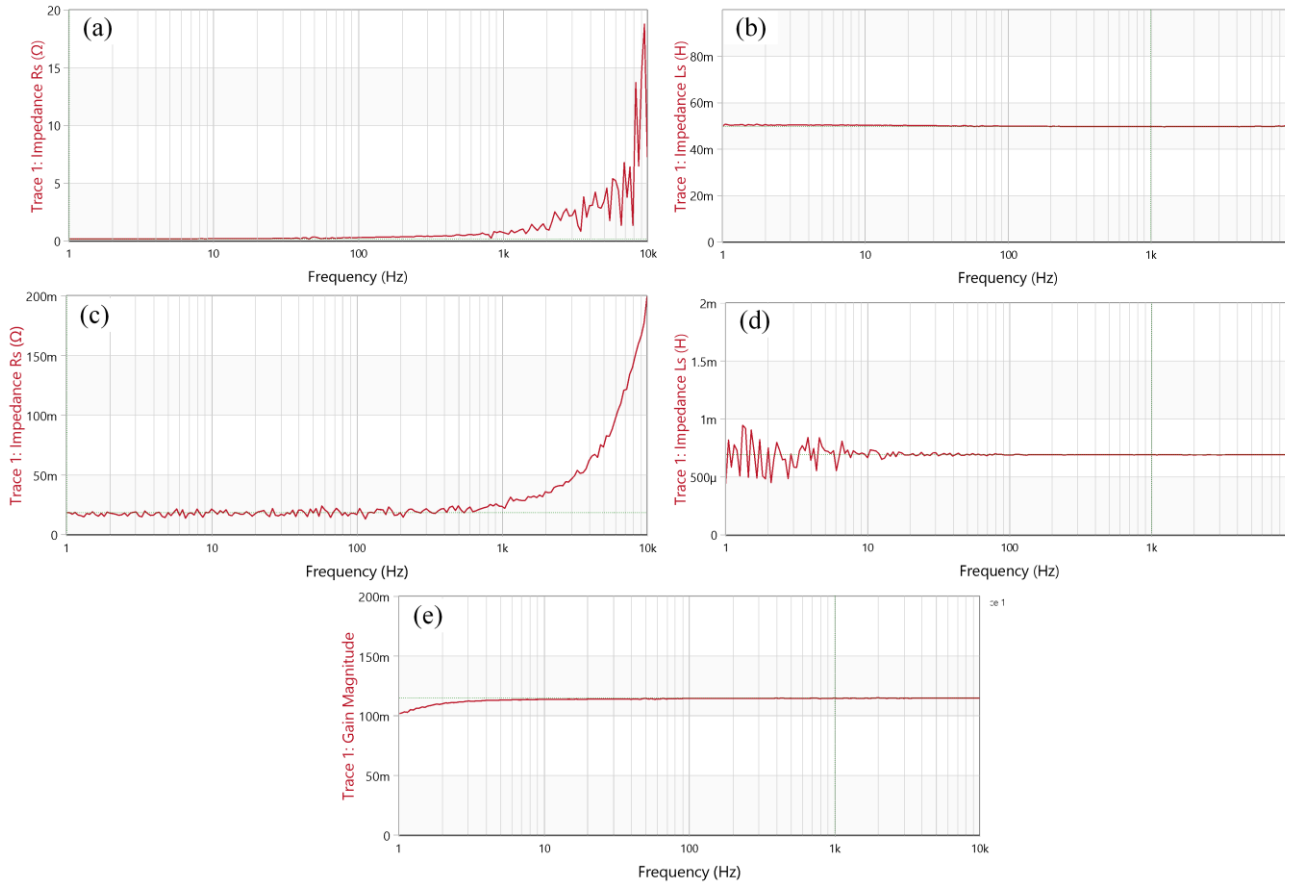

Fig. 10. The measurement results for phase 1 of the symmetrical transformer: a) parasitic resistance series in the primary side (R_1), b) inductance of the primary side (L_1), c) parasitic resistance series in the secondary side (R_2), d) inductance of the secondary side (L_2), and e) the gain (G).

conventional shell-type configuration.

REFERENCES

[1] D. K. Mishra *et al.*, "A review on solid-state transformer: A breakthrough technology for future smart distribution grids," *International Journal of Electrical Power & Energy Systems,* vol. 133, p. 107255, 2021.

[2] Z. Li, E. Hsieh, Q. Li, and F. C. Lee, "High-Frequency Transformer Design With Medium-Voltage Insulation for Resonant Converter in Solid-State Transformer," *IEEE Transactions on Power Electronics,* vol. 38, no. 8, pp. 9917-9932, 2023, doi: 10.1109/TPEL.2023.3279030.

[3] A. Anurag, S. Acharya, and S. Bhattacharya, "Solid state transformer for medium voltage grid applications enabled by 10 kv sic mosfet based three-phase converter systems," in *2021 IEEE 12th Energy Conversion Congress & Exposition-Asia (ECCE-Asia)*, 2021: IEEE, pp. 906-913.

[4] M. K. Kazimierczuk, D. Czarkowski, E. Institute of, and E. Electronics, *Resonant power converters*, 2nd ed. Hoboken, N.J.: IEEE, 2011.

[5] M. Noah, K. Umetani, S. Endo, H. Ishibashi, J. Imaoka, and M. Yamamoto, "A Lagrangian dynamics model of integrated transformer incorporated in a multi-phase LLC resonant converter," in *2017 IEEE Energy Conversion Congress and Exposition (ECCE)*, 1-5 Oct. 2017 2017, pp. 3781-3787, doi: 10.1109/ECCE.2017.8096668.

[6] S. A. Arshadi, M. Ordonez, W. Eberle, M. Craciun, and C. Botting, "Three-Phase LLC Battery Charger: Wide Regulation and Improved Light-Load Operation," *IEEE Transactions on Power Electronics,* vol. 36, no. 2, pp. 1519-1531, 2021, doi: 10.1109/TPEL.2020.3006422.

[7] R. L. Da Silva, V. L. F. Borges, C. E. Possamai, and I. Barbi, "Solid-state transformer for power distribution grid based on a hybrid switched-capacitor LLC-SRC converter: Analysis, design, and experimentation," *IEEE Access,* vol. 8, pp. 141182-141207, 2020.

[8] M. Noah *et al.*, "A novel three-phase LLC resonant converter with integrated magnetics for lower turn-off losses and higher power density," in *2017 IEEE Applied Power Electronics Conference and Exposition (APEC)*, 26-30 March 2017 2017, pp. 322-329, doi: 10.1109/APEC.2017.7930712.

[9] J. Zeng, G. Zhang, S. S. Yu, B. Zhang, and Y. Zhang, "LLC resonant converter topologies and industrial applications — A review," *Chinese Journal of Electrical Engineering,* vol. 6, no. 3, pp. 73-84, 2020, doi: 10.23919/CJEE.2020.000021.

[10] S. A. Arshadi, M. Ordonez, W. Eberle, M. A. Saket, M. Craciun, and C. Botting, "Unbalanced Three-Phase LLC Resonant Converters: Analysis and Trigonometric Current Balancing," *IEEE Transactions on Power Electronics,* vol. 34, no. 3, pp. 2025-2038, 2019, doi: 10.1109/TPEL.2018.2846526.

[11] Y. Nakakohara, H. Otake, T. M. Evans, T. Yoshida, M. Tsuruya, and K. Nakahara, "Three-Phase LLC Series Resonant DC/DC Converter Using SiC MOSFETs to Realize High-Voltage and High-Frequency Operation," *IEEE Transactions on Industrial Electronics,* vol. 63, no. 4, pp. 2103-2110, 2016, doi: 10.1109/TIE.2015.2499721.

[12] J. Cao, X. Zhang, P. Rao, S. Zhou, F. Zhou, and Q. Zhang, "Design of Three-Phase Delta-Delta LLC Resonant Converter," in *2020 IEEE Vehicle Power and Propulsion Conference (VPPC)*, 18 Nov.-16 Dec. 2020 2020, pp. 1-5, doi: 10.1109/VPPC49601.2020.9330918.

[13] C. Liao, J. Ruan, C. Liu, W. Wen, and Z. Du, "3-D Coupled Electromagnetic-Fluid-Thermal Analysis of Oil-Immersed Triangular Wound Core Transformer," *IEEE Transactions on Magnetics,* vol. 50, no. 11, pp. 1-4, 2014, doi: 10.1109/TMAG.2014.2330953.

[14] G. Upadhyay, A. Singh, S. K. Seth, and R. K. Jarial, "FEM based no-load loss calculation of triangular wound core transformer," in *2016 IEEE 1st International Conference on Power Electronics, Intelligent Control and Energy Systems (ICPEICES)*, 4-6 July 2016 2016, pp. 1-4, doi: 10.1109/ICPEICES.2016.7853594.

[15] A. Cervone, T. Wei, and D. Dujic, "Fourier-Based Harmonic Control of Plug-and-Play Active Filters for Input-Series/Output-Parallel Solid-State Transformers," in *IECON 2023- 49th Annual Conference of the IEEE Industrial Electronics Society*, 16-19 Oct. 2023 2023, pp. 1-8, doi: 10.1109/IECON51785.2023.10312149.

[16] Z. Lu, G. Xu, M. Su, Y. Liao, Y. Liu, and Y. Sun, "Stability Analysis and Design of Common Phase Shift Control for Input-Series Output-Parallel Dual Active Bridge With Consideration of Dead-Time Effect," *IEEE Journal of Emerging and Selected Topics in Power Electronics,* vol. 10, no. 6, pp. 7721-7732, 2022, doi: 10.1109/JESTPE.2022.3163286.

[17] H. Yu, Y. Shi, C. Wu, F. Wang, and C. Xu, "Input Series Output Parallel Phase-Shifted Full-Bridge Converter Design for Full Range Soft-Switching Effect and Minimum Output Current Ripple," in *2023 IEEE PELS Students and Young Professionals Symposium (SYPS)*, 27-29 Aug. 2023 2023, pp. 1-6, doi: 10.1109/SYPS59767.2023.10268189.

[18] R. Mirzadarani *et al.*, "Three-Phase Medium-Voltage Medium-Frequency Transformer for SST in Green Hydrogen Production," presented at the IECON 2023 - 49th Annual Conference of IEEE Industrial Electronics Society, Singapore, Singapore, 2023.

[19] M. Bitschnau, "Bode 100 - Application Note Transformer modelling," OMICRON Lab, 2017. [Online]. Available: https://www.omicron-lab.com/fileadmin/assets/Bode_100/ApplicationNotes/Transformer_modelling/App_Note_Transformer_modelling_V_2_0.pdf